Available online at www.sciencedirect.com

ScienceDirect

Procedia Engineering 5 (2010) 1328–1331

Procedia Engineering

www.elsevier.com/locate/procedia

Proc. Eurosensors XXIV, September 5-8, 2010, Linz, Austria

Modelling and evaluation of a thermal microfluidic sensor fabricated on plastic substrate

G. P. Patsis[a], A. Petropoulos[b], G. Kaltsas[a,*]

[a]*Department of Electronics, TEI of Athens, Athens, Greece*
[b]*Institute of Microelectronics NCSR Demokritos, Athens, Greece*

Abstract

Both the simulation and the experimental evaluation of a thermal microfluidic flow sensor are presented in this work. The sensor was evaluated in the calorimetric principle of operation with water as the test liquid. The simulation of the sensor operation was performed into the framework of Comsol® software package. Various combinations of microchannel geometries were tested with different input flow rate values. The operational parameters of the device were simulated by 3D models. The dominant operation parameter was determined to be the distance of the upstream-downstream sensing elements to the heater, the effect of which was theoretically extracted and experimentally verified.

Thermal microfluidic sensor; modelling; plastic substrate

1. Introduction

This work presents the experimental evaluation and the numerical simulation of a microfluidic flow sensor. The device was fabricated utilizing an innovative technology which allows direct integration of microstructures on organic substrates [1,2]. It consists of a micro-channel integrated on top of an array of temperature sensitive Pt elements, which are directly connected to the copper tracks of a PCB. The micro-channel was fabricated by SU8 which allows the formation of structures of highly controllable thickness-to-width ratio. The microchannel sealing was performed by a commercial 3M tape. Fig.1 illustrates the main parts of the device as well as the inlet-outlet configuration.

Nomenclature

ρ	fluid's density (kg/m^3)
$\vec{u}$	velocity vector (m/s)
p	pressure (Pa)

1877-7058
doi:10.1016/j.proeng.2010.09.359

η	dynamic viscosity (Pa s)
$\vec{F}$	body force term (N/m^3)
$\vec{I}$	unity matrix
C_p	specific heat capacity at constant pressure (J/(kg m))
T	absolute temperature (K)
T_{amb}	ambient absolute temperature (K)
k	thermal conductivity (W/(m K))
g_0	acceleration due to gravity (m/s^2)
$(\nabla u)^T$	velocity gradient transpose matrix
$\hat{x}$, $\hat{y}$, $\hat{z}$	unit vectors in the three normal Cartesian axes.

The sensor was evaluated in the calorimetric principle of operation [3], whereby the temperature distribution in pre-specified locations in either side of a heater is monitored as a function of the flow. The Pt elements (Fig.1) can act either as heaters by applying external power to them, or as sensing elements by monitoring the corresponding resistance changes. In the calorimetric operating principle, a certain Pt element acts as a heating source, while two other elements, situated on opposite heater sides, are used to detect the flow-induced temperature differences. The response of the sensor is mainly affected by two parameters: the microchannel cross-sectional area and the combination of the upstream-downstream sensing distance.

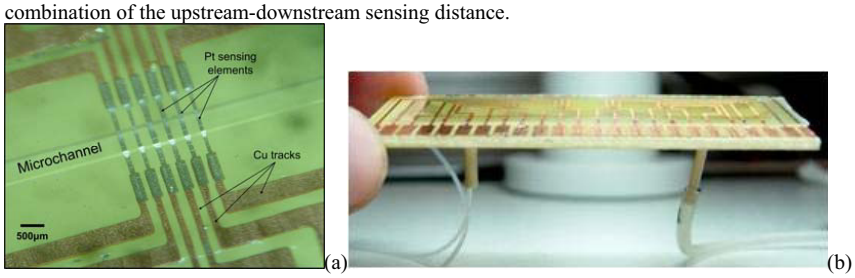

Fig. 1: (a) Top-down view of the sensor where the heater, the temperature sensors and the micro-channel are shown (b) Side view of the device.

2. Model Description and Comparison with Experimental Results

The device simulation was performed with the Comsol® package [4]. In order to achieve accurate representation of the existing structure, the developed models were three dimensional. In each case, a specific model corresponding to a certain experimental configuration required different boundary conditions, while the study was focused mainly on the effect of the width and the height of the microchannel crossection on the sensor performance. Regarding each model, the corresponding temperature field near the heater was extracted as a function of predefined input flows in order to obtain the theoretical sensor response and therefore providing information regarding the subsequent tuning of the design geometry in order to enhance the device performance. Water was considered as the fluid in the microchannel. A schematic representation of the microchannel is shown in Fig. 2(a) while an example of the simulation results regarding the temperature distribution in the entire microchannel for a certain input flow rate is provided in Fig. 2(b).

The developed models are based on the Navier-Stokes equations for the description of flow in viscous fluids with momentum balance for each component of the momentum vector in all spatial dimensions. They also assume that the density and viscosity of the modelled fluid are constant, an assumption compatible to the continuity condition. A certain formulation of the aforementioned system of equations termed the weakly compressible Navier-Stokes equations, are suitable when small density variations arise due to temperature differences. They are not suitable for high velocities or when fluid compression/expansion results in substantial internal work or heat effects. In the total stress tensor formulation and taking into consideration the incompressibility assumption they are:

$$\rho(\vec{u}\cdot\nabla)\vec{u} = \nabla\cdot\left[p\vec{I} + \eta\left(\nabla\vec{u} + (\nabla\vec{u})^T\right)\right] = \vec{F},\ \nabla\vec{u} = 0 \tag{1}$$

The heat equation is given by the following formula:

$$\nabla\cdot(-k\nabla T) = -\rho C_p\vec{u}\cdot\nabla T \tag{2}$$

Fluid velocity is the variable in both equations, while temperature is found in the buoyancy term:

$$\vec{F} = \left\{0\hat{x}, 0\hat{y}, a(T)g_0\rho(T)(T - T_{amb})\hat{z}\right\} \tag{3}$$

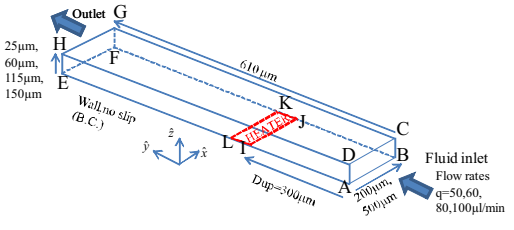

(a)

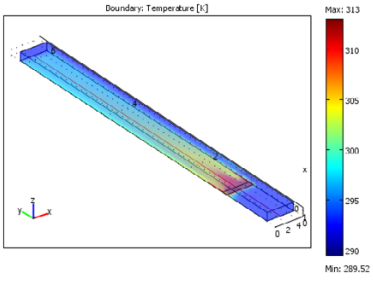

(b)

Fig. 2: (a) Simulated geometry. (b) Simulation of temperature distribution in microchannel of 500μm width, 150μm height for inlet flow q=50μl/min.

Table 1. Boundary settings for Incompressible Navier – Stokes equations. Table 2. Boundary Settings for Heat Transfer (Conduction – Diffusion) Equation. B.T. is Boundary Type and B.C. is Boundary Condition.

Incompressible Navier – Stokes Equation				Heat Transfer (Conduction – Diffusion) Equation			
FACE	**B.T.**	**B.C.**	**EQUATION**	**FACE**	**B.T.**	**B.C.**	**EQUATION**
ABCD	Inlet	Velocity	$\vec{u} = U_0\hat{y}$	ABCD	Inlet	Temperature	$T = T_{inf} = 293^o K$
EFGH	Outlet	Pressure, no viscous stress	$-\eta\left(\nabla\vec{u} + (\nabla\vec{u})^T\right)\hat{y} = \vec{0},$ $p = 0$	EFGH	Outlet	Temperature	$T = T_{inf} = 293^o K$
EADH	Wall	No slip	$\vec{u} = 0$	EADH	Wall	Thermal insulation	$\hat{y}(-k\nabla T) = 0$
FBCG	Wall	No slip	$\vec{u} = 0$	FBCG	Wall	Thermal insulation	$\hat{y}(-k\nabla T) = 0$
HDCG	Wall	No slip	$\vec{u} = 0$	HDCG	Wall	Thermal insulation	$\hat{y}(-k\nabla T) = 0$
HABF	Wall	No slip	$\vec{u} = 0$	IABJ	Wall	Thermal insulation	$\hat{y}(-k\nabla T) = 0$
				ELKF	Wall	Thermal insulation	$\hat{y}(-k\nabla T) = 0$
				LIJK	Heater	Temperature	$T = T_{heater} = 313^o K$

In this mode the density, the dynamic viscosity and the body force term (the buoyancy change due to temperature variations above the heater) can be defined as a function of any other dependent variables; in this case as a function of temperature in the microchannel. Typically, this mode could be coupled to the heat equation where the density is a function of temperature, which is the case in this work. The coupled system of equations is then solved simultaneously. To fully define the problem, boundary conditions are needed for the flow and temperature on the channel boundaries. Table 1 shows the boundary conditions for the incompressible Navier-Stokes equations and for the heat transfer equation.

According to the extracted numerical results the dominant geometrical parameter regarding sensor performance is the micro-channel height, while the channel width was found to only slightly affect the sensor response. Fig. 3

shows the temperature as a function of position along the channel length (y) at the bottom of the micro-channel with W = 500 μm for various heights (H) and for a constant flow rate of q=50μl/min.

The specific behavior was experimentally proved as shown in Fig.4, where the sensor response as a function of flow is shown for two different micro-channel widths (W=200 μm and W=500 μm) and for channel height H=115 μm. On the same graph the theoretical result for the corresponding W=500 μm wide micro-channel is also superimposed. The temperature difference corresponds to sensing elements (upstream and downstream) situated symmetrically with respect to the heater in a distance of 300μm. A satisfactory agreement is observed although small deviations exist between the absolute values of the theoretical and the experimental data, as expected.

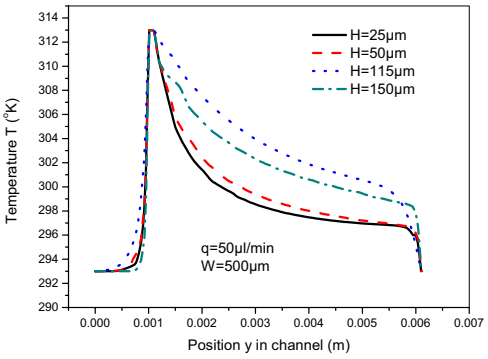

Fig.3: Temperature vs. position along the channel length (y) at the bottom of the microchannel, for flow rate q=50μl/min. The channel width is (a) W = 200 μm and (b) W = 500 μm respectively.

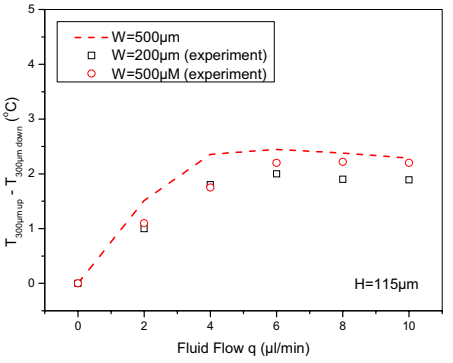

Fig. 4: The experimental sensor response as a function of flow for two different microchannel widths. The height of the micro-channel is 115μm. The upstream and downstream distance of the sensing elements is 300μm. The corresponding theoretical response is also added for comparison.

References

[1] K. Kontakis, A. Petropoulos, G. Kaltsas, T. Speliotis, E. Gogolides, Microelectronic Engineering 86 (2009) 1382-1384.

[2] A. Petropoulos, D. Goustouridis, T. Speliotes, G. Kaltsas, European Physical Journal - Applied Physics, 46 (2009) 12507.

[3] B. W. van Oudheusden, “Silicon thermal flow sensors”, Sensors and Actuators A 30 (1992) 5-26.

[4] www.comsol.com.